

Wavelength-resolved stimulated photon echoes: Direct observation of ultrafast intramolecular vibrational contributions to electronic dephasing

Lewis D. Book and Norbert F. Scherer^{a)}

Department of Chemistry, The James Franck Institute and the Institute for Biophysical Dynamics,
5735 South Ellis Avenue, University of Chicago, Chicago, Illinois 60637

(Received 22 December 1998; accepted 13 May 1999)

Novel wavelength-resolved stimulated photon echo measurements on a dye molecule in solution are presented. Data are simulated within the multimode Brownian oscillator model using the spectral density of de Boeij *et al.* [J. Phys. Chem. **100**, 11806 (1996)] for the same solute–solvent system. For photon echo population times < 50 fs there are considerable differences between the measured and calculated data. Aided by further simulations, we conclude that these discrepancies result from dephasing dynamics of high frequency intramolecular vibrational modes not included in the previously derived spectral density. © 1999 American Institute of Physics.
[S0021-9606(99)51427-X]

A central problem in the study of chemical reactivity in condensed phase environments is the determination of the colored noise spectrum that describes the fluctuating interactions between a chromophore and its surrounding “bath.”¹ In recent years, femtosecond photon echo spectroscopy has been widely employed to investigate chromophore-bath dynamics in solutions^{2–4} and other condensed phase environments.^{5,6} Photon echoes and other nonlinear optical spectroscopies have often been interpreted within the multimode Brownian oscillator model.⁷ In this theory, a chromophore-solvent system is modeled as a two-level electronic system linearly coupled to a bath of harmonic oscillators corresponding to both chromophore and solvent nuclear degrees of freedom.

A key component of the Brownian oscillator model is the correlation function $M(t)$ for the energy gap between the two electronic levels, defined as⁷

$$M(t) = \frac{\langle \Delta \omega_{eg}(0) \Delta \omega_{eg}(t) \rangle}{\langle \Delta \omega_{eg}^2 \rangle}, \quad (1)$$

where $\Delta \omega_{eg}$ is the bath-induced fluctuation of a chromophore’s transition frequency away from the average $\langle \omega_{eg} \rangle$. There is a direct relationship between a system’s $M(t)$ and its spectral density.⁷ All resonant linear and nonlinear optical response functions can be calculated with knowledge of this correlation function and two static coupling parameters. Because $M(t)$ contains considerable information about the dynamics of a chromophore-solvent system, and because its relationship to experimental observables is well-defined, considerable effort has been expended on determining $M(t)$ for a wide range of systems.^{3–6}

Among the highest quality energy gap correlation functions available are those determined by de Boeij *et al.* for the dye molecule DTTCI (3,3’-diethylthiatricarbocyanine iodide) in ethylene glycol, methanol, and acetonitrile

solutions.³ These $M(t)$ ’s provide good fits to several independent measurements: three-pulse stimulated photon echo, time-gated photon echo, and transient grating data, as well as portions of the linear absorption and emission spectra. An interesting feature of these correlation functions is that they contain an initial rapidly decaying component that causes the correlation function to decay to about half of its initial value in about 30 fs. This ultrafast loss of correlation was attributed to “a free induction-like decay produced by excitation of vibrational structure across the whole absorption band.”³ A large molecule like DTTCI has a near-continuum of vibrational states at higher vibrational energies, many of which will be coupled (if only weakly) to the molecule’s electronic transitions. It seems reasonable that these modes would manifest themselves as a rapid decay in the initial dephasing dynamics of the chromophore following excitation with a broadband optical pulse. This assignment has not yet been firmly established because it has not been possible to obtain direct information on the mechanism for such fast dynamics (nearly equal to the pulse width).

This letter presents experimental and calculated wavelength-resolved stimulated photon echo (WRSPE) signals for DTTCI in methanol. The experimental data provide direct evidence that the initial dephasing dynamics of this system include a significant component due to a collection of states that lie above the chromophore’s 0–0 transition, i.e., intramolecular vibrational modes. Calculations are presented that show that the correlation function of de Boeij *et al.*³ does not capture these dynamics. This is attributed to the fact that their $M(t)$ only explicitly includes a few high frequency modes with relatively long dephasing times. We argue that it will be necessary to model more accurately both the spectrum of high frequency modes coupled to the optical excitation and the mechanism that dephases them in order to account for our experimental measurements.

The third-order electronic polarization that induces the photon echo signal is given by⁷

^{a)} Author to whom correspondence should be addressed. Electronic mail: nscherer@rainbow.uchicago.edu

$$P^{(3)}(t, T_{12}, T_{23}) \propto \int_0^\infty dt_1 \int_0^\infty dt_2 \int_0^\infty dt_3 E_1^*(t-t_3-t_2-t_1) \times E_2(t-t_3-t_2) E_3(t-t_3) R^{(3)}(t_3, t_2, t_1), \quad (2)$$

where E_1 , E_2 , and E_3 are the electric fields of the three applied pulses, T_{12} and T_{23} are the time delays between the first and second, and second and third pulses, respectively, and $R^{(3)}$ is the third-order nonlinear optical response function. In the rotating wave approximation (valid in electronically resonant measurements), $R^{(3)}$ is the sum of 16 Feynman diagram pathways in the Liouville space density matrix formalism.⁷ For a stimulated photon echo measurement, the coherence time T_{12} is scanned for a fixed population time T_{23} . The detected signal at a given set of T_{12} and T_{23} times is the modulus square of $P^{(3)}$ integrated over all time t . Hence, knowledge of the temporal shape of the nonlinear polarization is lost. This information can be recovered in the time-gated photon echo (TGPE) measurement, where the third-order polarization is up-converted in a noncentrosymmetric crystal with a reference or “gating” pulse.⁸ Assuming a delta-function gating pulse $\delta(t-t_g)$, the TGPE signal is

$$S_{\text{TGPE}}(t_g, T_{23}, T_{12}) \propto |P^{(3)}(t_g, T_{23}, T_{12})|^2. \quad (3)$$

The TGPE thus measures the intensity profile of the photon echo polarization. Given a constant value of T_{23} , the intensity of this polarization evolves rapidly as a function of T_{12} and is therefore very sensitive to short-time dynamics. Unfortunately, this measurement is difficult to implement experimentally because it requires the rather weak echo signal to be used as an input beam in a sum-frequency mixing process.⁸

Another possible way to obtain information about the photon echo polarization that avoids an up-conversion step is to spectrally disperse the signal with a monochromator and detect it as a function of wavelength rather than time. For a monochromator with a spectral response of $\delta(\lambda-\lambda_D)$, the WRSPE signal is given by

$$S_{\text{WRSPE}}(\lambda_D, T_{23}, T_{12}) \propto \left(\frac{2\pi c}{\lambda_D}\right)^2 |P^{(3)}(\lambda_D, T_{23}, T_{12})|^2, \quad (4)$$

where λ_D is the detection wavelength and c is the speed of light. Wegener and co-workers recently used this type of measurement to investigate exciton dynamics in GaAs.⁹ While the TGPE and the WRSPE arise from the same nonlinear polarization, they cannot be analytically related to each other by Fourier transformation. This is because the modulus squaring that occurs in both measurements results in the loss of phase information in both the time and wavelength domains. Heterodyne-detected photon echo methods bridge this gap but are considerably more involved.¹⁰

The ultrafast pulses used in the present measurements were produced by a home-built, cavity-dumped Ti:sapphire laser¹¹ operating at 16 kHz that produces nearly chirp-free pulses of 14 fs (Gaussian FWHM) duration centered at 795 nm. The output of this laser was split into three portions and each of the resulting beams (~ 4 nJ/pulse) was sent down variable (beams E_1 and E_3) or fixed (E_2) optical delay lines

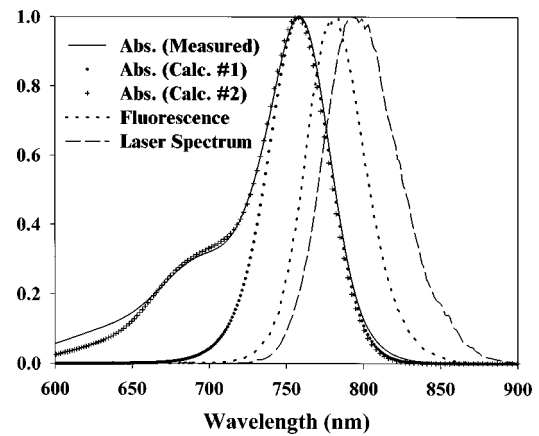


FIG. 1. Measured absorption spectrum of DTTCl in methanol, absorption spectrum calculated with the parameters given in Ref. 3, absorption spectrum calculated as described in the text, measured fluorescence spectrum, and the spectrum of the ultrafast pulses used in photon echo measurements described in the text. The fluorescence spectrum is corrected for solution reabsorption.

prior to being focused into the sample. The sample (peak optical density of 0.25) was contained in a 500 μm path-length spinning cell. For a given WRSPE measurement, the T_{23} time was fixed by setting the path length of the E_3 beam to the appropriate delay and scanning the T_{12} time from -70 to 100 fs. The stimulated photon echo signal in the phase-matched $\mathbf{k}_s = \mathbf{k}_3 + \mathbf{k}_2 - \mathbf{k}_1$ direction was sent through a 1/8-m monochromator (4 nm bandpass) and individual spectral components were detected with an avalanche photodiode. A detailed description of the experimental setup will be given in a forthcoming paper.¹²

Figure 1 shows the measured absorption spectrum for the DTTCl/methanol solution, the absorption spectrum calculated from the parameters given in Ref. 3, an absorption spectrum calculated as described below, the measured fluorescence spectrum of this solution, and the laser spectrum used in the photon echo experiments. Contour plots of WRSPE signals from the solution are shown in Figs. 2(a)–2(c) for T_{23} values of 0, 30, and 250 fs. The first observation to be made is that the signal evolves from an irregular shape at $T_{23}=0$ fs to a nearly elliptical shape by $T_{23}=250$ fs. The most prominent change from one plot to another is that the short wavelength “tail” that protrudes from the $T_{23}=0$ fs signal decays rapidly with increasing T_{23} time; the outermost contour (5% of signal maximum) extends below 730 nm at $T_{23}=0$ fs and reaches only 740 nm by $T_{23}=30$ fs. By $T_{23}=50$ fs (not shown) this tail feature has almost completely disappeared.

Plots in Figs. 2(d)–2(f) show simulated WRSPE signals that correspond to the experimental data of Figs. 2(a)–2(c). These plots were calculated numerically using Eqs. (2) and (4) using the $M(t)$ and coupling constants reported for the DTTCl/methanol solution.³ Like the experimental signal, the simulated one transforms from an irregular shape at $T_{23}=0$ to a near-perfect ellipse by $T_{23}=250$ fs. For wavelengths greater than 760 nm there are similarities between the measured and calculated signals; the $T_{23}=250$ fs results are in fact in fairly good agreement throughout the detected spectral range. However, the calculated WRSPEs lack the dis-

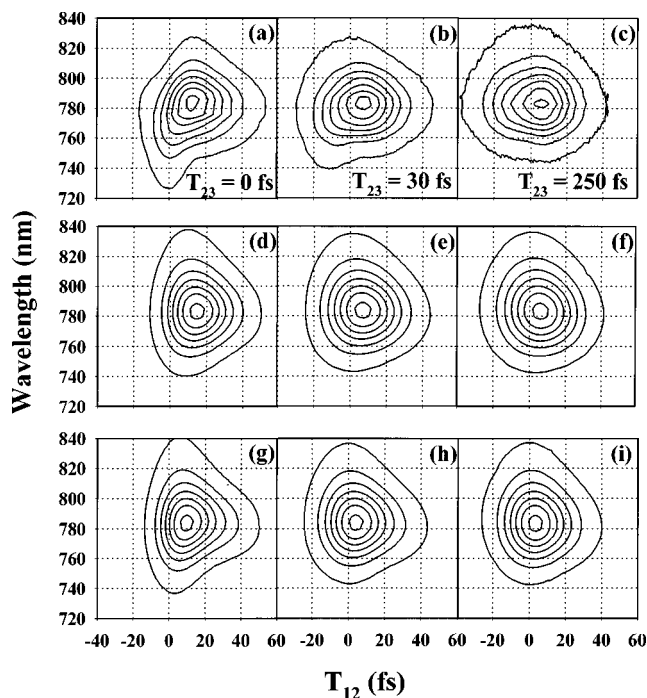


FIG. 2. (a)–(c) Experimental wavelength-resolved stimulated photon echo signals of DTTCl/methanol for the T_{23} times 0, 30, and 250 fs, respectively. (d)–(f) Calculated signals corresponding to the experimental data presented in (a)–(c). The response function needed to calculate these signals was determined from the $M(t)$ correlation function and other parameters given in Ref 3. (g)–(i) Calculated signals as in (d)–(f) but with $M(t)$ modified as explained in the text. The peak value of each plot in this figure is normalized to one. The value of the signal at the outermost contour is 0.05. The value at each successively inner contour increases by 0.15.

tinctive feature below 760 nm present in the experimental data for $T_{23}=0$ and 30 fs.

The presence of a short-time feature in the measured WRSPE signals that is not predicted by the calculations can be explained by two possibilities. Either the experimental data contains contributions from sources other than that of the resonant third-order response of the solution, or the spectral density modeling the system does not adequately reflect its true optical response. One source of artifacts in the experimental signals could be contributions from fifth-order effects.¹³ This is ruled out by power dependent measurements where the same results are obtained when the per-pulse energy was varied by a factor of four. Another possibility is that a nonresonant contribution from the solvent is detected along with the signal from the chromophore. The much weaker third-order signal from neat methanol can be detected from below 700 nm to above 900 nm, reflecting the bandwidth of the optical pulses.¹² If the tail features in Fig. 2 were due to the solvent, a comparably sized signal would be seen at wavelengths greater than 830 nm. Because this is not observed, and because the WRSPE and solvent scattering signals are differently shaped, we conclude that the nonresonant response from the solvent is negligible. Chirped pulses can induce unusual effects in ultrafast optical signals around the zero of time.¹⁴ However, unrealistically large amounts of chirp are required in the calculations in order to produce signals that even remotely resemble the experimental data. Since the pulses used in the experiments are nearly chirp-

free, as established by transient-grating frequency-resolved optical gating measurements,^{12,15} this explanation can be ruled out.

As noted above, in the WRSPE for $T_{23}=0$ fs [Fig. 2(a)] a portion of the signal ($\lambda < 760$ nm) that is centered nearly at $T_{12}=0$ fs decays away rapidly as T_{23} is increased, i.e., by $T_{23}=50$ fs. A relaxation time of this magnitude (tens of femtoseconds) is much too fast to be due to conventional solvation dynamics for such a weakly solvating system.¹⁶ A dephasing mechanism operative on this time scale would likely involve the intramolecular vibrational modes of DTTCl. Because the bandwidth of the optical pulses used in the present measurements exceeds 1000 cm^{-1} , a considerable range of vibrational frequencies may be excited in the both the ground and excited states of the chromophore via resonance Raman-type processes and linear electron–nuclear coupling, respectively.¹⁷ Although a resonance Raman spectrum of DTTCl is not available, such data from other carbocyanine dyes indicate that the electronic transitions of these chromophores are coupled to a broad band of nuclear modes, especially at frequencies greater than $\sim 700\text{ cm}^{-1}$.¹⁸ Following impulsive optical excitation, this quasicontinuum of vibrational modes could induce very rapid electronic dephasing due to the effect of superposing a large number of oscillators with a wide range of incommensurate frequencies. This superposition could result in a very rapid initial loss of correlation.

Ultrafast dephasing processes involving high frequency vibrational modes are not directly accounted for in the correlation function of de Boeij *et al.*³ Instead, they are modeled by the inclusion of a rapidly decaying Gaussian component (time constant of 14 fs) in $M(t)$. While this function was sufficient to model wavelength-integrated photon echoes, it predicts an absorption spectrum that falls off too quickly on its blue edge compared to the experimental spectrum (Ref. 3 and Fig. 1). This is due to the fact that this spectral density contains insufficient vibronic coupling at shorter wavelengths. This is also a likely explanation for the discrepancies between this model and our wavelength-resolved measurements, which occur most prominently in the shorter wavelength region of the spectrum.

As a first attempt to take into account the influence of a dense manifold of high frequency vibrational modes on our WRSPE's, we have modified the previously derived $M(t)$. The ultrafast Gaussian component was removed and replaced with a quasicontinuum of 640 Brownian oscillators with frequencies ranging from 0 to 2000 cm^{-1} equally spaced with intervals of 3.125 cm^{-1} . The coupling parameter $\lambda(\omega)$ for each mode of frequency ω was determined by the expression $\lambda_0 \exp[-(\omega - \omega_0)^2/2\sigma^2]$, where $\lambda_0 = 1.2\text{ cm}^{-1}$, $\omega_0 = 1300\text{ cm}^{-1}$, and $\sigma = 636\text{ cm}^{-1}$. This form for $\lambda(\omega)$ crudely accounts for the fact that the density of states rises steeply as a function of vibrational energy while the Franck–Condon factors fall off sharply for an electronic transition that is coupled to an increasingly greater change in vibrational quantum number.¹⁹ Addition of these modes provides an improved fit to the higher energy side of the absorption spectrum (Fig. 1). A resonance Raman spectrum would

provide a better constraint on the choice of parameters.²⁰ Calculated WRSPE signals using this new $M(t)$ are shown in Figs. 2(g)–2(i) for $T_{23}=0, 30,$ and 250 fs. Comparing Fig. 2(g) to 2(a) and 2(d), it can be seen that the vibrational manifold improves the fit between simulation and experiment for wavelengths below 760 nm, although the correspondence is still somewhat unsatisfactory. The new modes have small but noticeable effects at larger T_{23} times. Simulations with equal displacements for all modes or with less than 100 modes gave inferior results to those shown here.

It is appropriate to consider another possible interpretation of our experimental data. The ultrafast decay of the signal below 760 nm in Fig. 2(a) could be due to vibrational population relaxation and redistribution to lower energy levels through anharmonic couplings of the initially excited states to the whole range nuclear states of the chromophore and perhaps strongly coupled solvent molecules. This process would be analogous to picosecond intramolecular vibrational-energy redistribution (IVR) observed by Felker and Zewail in ultracold, isolated large molecules.²¹ Because the bandwidth of the pulses employed in the present measurements is broader by three orders-of-magnitude, a correspondingly broader distribution of states can be accessed, resulting in correspondingly faster wavepacket dephasing and perhaps also dissipation. While it has not been definitively established, several groups have indirectly inferred IVR time scales for large organic dye molecules (similar to DTTCI) in solution of a few tens of femtoseconds or less.^{14,22–24} Simulation of such dynamics would require the use of a model that includes vibrational population relaxation,^{25,26} which is not taken into account in the standard Brownian oscillator model.

Other effects not included in the Brownian oscillator model may be important.²⁷ For example, there are indications that DTTCIs S_0 and S_1 potential surfaces may be significantly different. This is suggested by the fact that the absorption and emission spectra do not exhibit mirror symmetry.²⁸ Also, this condition might explain why the $T_{23}=0$ fs simulations [Figs. 2(d), 2(g)] overestimate the WRSPE signal at wavelengths greater than 820 nm.¹²

In conclusion, it has been shown that by wavelength resolving the stimulated photon echo signal for a dye molecule in solution short-time dynamics are observed that are not apparent in time-gated or other wavelength-integrated photon echoes. In conjunction with simulations, these measurements indicate the importance of properly considering the complete range nuclear motion involved in the initial electronic dephasing dynamics of a chromophore-bath system. Obtaining quantitative agreement between experiment and calculation may require relaxing approximations usually made when employing the multimode Brownian oscillator model.

We acknowledge Dr. David Arnett for his essential role in the development of the experimental apparatus. This work was supported by the National Science Foundation (CHE-9357424), the National Institutes of Health (RO1-8M57768) and the Packard, Dreyfus, and Sloan Foundations.

- ¹S. Dattagupta, *Relaxation Phenomena in Condensed Matter Physics* (Academic, New York, 1987).
- ²P. Vöhringer, D. C. Arnett, R. A. Westervelt, M. J. Feldstein, and N. F. Scherer, *J. Chem. Phys.* **102**, 4027 (1995); T.-S. Yang, P. Vöhringer, D. C. Arnett, and N. F. Scherer, *ibid.* **103**, 8346 (1995).
- ³W. P. de Boeij, M. S. Pshenichnikov, and D. A. Wiersma, *J. Phys. Chem.* **100**, 11806 (1996).
- ⁴T. Joo, Y. Jia, J.-Y. Yu, M. J. Lang, and G. R. Fleming, *J. Chem. Phys.* **104**, 6089 (1996); S. A. Passino, Y. Nagasawa, and G. R. Fleming, *ibid.* **107**, 6094 (1997).
- ⁵T. Joo, Y. Jia, J.-Y. Yu, D. M. Jonas, and G. R. Fleming, *J. Phys. Chem.* **100**, 2399 (1996).
- ⁶Y. Nagasawa, J.-Y. Yu, and G. R. Fleming, *J. Chem. Phys.* **109**, 6175 (1998).
- ⁷S. Mukamel, *Principles of Nonlinear Optical Spectroscopy* (Oxford University, New York, 1995); Y. J. Yan and S. Mukamel, *J. Chem. Phys.* **94**, 179 (1991).
- ⁸P. Vöhringer, D. C. Arnett, T.-S. Yang, and N. F. Scherer, *Chem. Phys. Lett.* **237**, 387 (1995); M. S. Pshenichnikov, K. Duppen, and D. A. Wiersma, *Phys. Rev. Lett.* **74**, 674 (1995).
- ⁹M. U. Wehner, D. Steinbach, and M. Wegener, *Phys. Rev. B* **54**, R5211 (1996), and references therein.
- ¹⁰S. M. Gallagher, A. W. Albrecht, J. D. Hybl, B. L. Landin, B. Rajaram, and D. M. Jonas, *J. Opt. Soc. Am. B* **15**, 2338 (1998).
- ¹¹A. Baltuška, Z. Wei, M. S. Pshenichnikov, D. A. Wiersma, and R. Szipöcs, *Appl. Phys. B: Lasers Opt.* **65**, 175 (1997); B. N. Flanders, D. C. Arnett, and N. F. Scherer, *IEEE J. Sel. Top. Quantum Electron.* **4**, 353 (1998).
- ¹²L. D. Book, D. C. Arnett, and N. F. Scherer (unpublished).
- ¹³T. Joo, Y. Jia, and G. R. Fleming, *J. Chem. Phys.* **102**, 4063 (1995).
- ¹⁴S. H. Ashworth, T. Hasche, M. Woerner, E. Riedle, and T. Elsaesser, *J. Chem. Phys.* **104**, 5761 (1996).
- ¹⁵J. N. Sweetser, D. N. Fittinghoff, and R. Trebino, *Opt. Lett.* **22**, 519 (1997).
- ¹⁶M. L. Horng, J. A. Gardecki, A. Papazyan, and M. Maroncelli, *J. Phys. Chem.* **99**, 17311 (1995).
- ¹⁷A. E. Johnson and A. B. Myers, *J. Chem. Phys.* **104**, 2497 (1996).
- ¹⁸M. R. Kagan and R. L. McCreery, *Anal. Chem.* **66**, 4159 (1994); S. H. Ashworth, A. Kummrow, and K. Lenz, *J. Raman Spectrosc.* **28**, 537 (1997).
- ¹⁹B. R. Henry and W. Siebrand, *Organic Molecular Photophysics*, edited by J. B. Birks (Wiley, London, 1973), Vol. 1, p. 153.
- ²⁰M. K. Lawless and R. A. Mathies, *J. Chem. Phys.* **96**, 8037 (1992).
- ²¹P. M. Felker and A. H. Zewail, *J. Chem. Phys.* **82**, 2975 (1985).
- ²²G. Angel, R. Gagel, and A. Laubereau, *Chem. Phys.* **131**, 129 (1989); *Chem. Phys. Lett.* **156**, 169 (1989).
- ²³A. J. Taylor, D. J. Erskine, and C. L. Tang, *Chem. Phys. Lett.* **103**, 430 (1984); M. J. Rosker, F. W. Wise, and C. L. Tang, *Phys. Rev. Lett.* **57**, 321 (1986).
- ²⁴I. Martini and G. V. Hartland, *J. Phys. Chem.* **100**, 19764 (1996).
- ²⁵K. Shan, Y. J. Yan, and S. Mukamel, *J. Chem. Phys.* **87**, 2021 (1987); R. F. Loring, Y. J. Yan, and S. Mukamel, *ibid.* **87**, 5840 (1987).
- ²⁶S. H. Lin, *J. Chem. Phys.* **61**, 3810 (1974); M. Hayashi, T.-S. Yang, A. Mebel, C. H. Chang, S. H. Lin, and N. F. Scherer, *Chem. Phys.* **217**, 259 (1997).
- ²⁷Y. Zhao, V. Chernyak, and S. Mukamel, *J. Phys. Chem. A* **102**, 6614 (1998).
- ²⁸J. B. Birks and D. J. Dyson, *Proc. R. Soc. London* **A275**, 135 (1963).